Contrib Mineral Petrol (2001) 140: 458–468 © Springer-Verlag 2001

Daniela Rubatto · Ian S. Williams · Ian S. Buick

# Zircon and monazite response to prograde metamorphism in the Reynolds Range, central Australia

Received: 7 April 2000 / Accepted: 12 August 2000

**Abstract** We report an extensive field-based study of zircon and monazite in the metamorphic sequence of the Reynolds Range (central Australia), where greenschist- to granulite-facies metamorphism is recorded over a continuous crustal section. Detailed cathodoluminescence and back-scattered electron imaging, supported by SHRIMP U–Pb dating, has revealed the different behaviours of zircon and monazite during metamorphism. Monazite first recorded regional metamorphic ages (1576 ± 5 Ma), at amphibolite-facies grade, at ~600 °C. Abundant monazite yielding similar ages (1557 ± 2 to 1585 ± 3 Ma) is found at granulite-facies conditions in both partial melt segregations and restites. New zircon growth occurred between 1562 ± 4 and 1587 ± 4 Ma, but, in contrast to monazite, is only recorded in granulite-facies rocks where melt was present (≥700 °C). New zircon appears to form at the expense of pre-existing detrital and inherited cores, which are partly resorbed. The amount of metamorphic growth in both accessory minerals increases with temperature and metamorphic grade. However, new zircon growth is influenced by rock composition and driven by partial melting, factors that appear to have little effect on the formation of metamorphic monazite. The growth of these accessory phases in response to metamorphism extends over the 30 Ma period of melt crystallisation (1557–1587 Ma) in a stable high geothermal regime. Rare earth element patterns of zircon overgrowths in leucosome and restite indicate that, during the protracted metamorphism, melt-restite equilibrium was reached. Even in the extreme conditions of long-lasting high temperature (750–800 °C) metamorphism, Pb inheritance is widely preserved in the detrital zircon cores. A trace of inheritance is found in monazite, indicating that the closure temperature of the U–Pb system in relatively large monazite crystals can exceed 750–800 °C.

Supplementary Tables 1–2 are part of electronic supplementary material only. They have been deposited in electronic from and can be obtained from http://link.springer.de/link/service/journals/00410.

D. Rubatto (✉) · I. S. Williams
Research School of Earth Sciences,
Australian National University, Canberra,
ACT 0200, Australia
e-mail: daniela.rubatto@anu.edu.au

I. S. Buick
School of Earth Sciences and VIEPS,
La Trobe University, Bundoora,
Victoria 3038, Australia

Editorial responsibility: J. Hoefs

## Introduction

The reconstruction of the pressure–temperature–time (P–T–t) evolution of crustal sections is fundamental to understanding many tectonic processes. This task, particularly difficult in the case of polymetamorphic rocks, requires the combination of metamorphic petrology and geochronology of different mineral phases that potentially can record more than one geological event. Zircon and monazite have been largely used for this role in high-grade terrains because their U–Pb system is able to retain the memory of polyphase evolution even at relatively high temperatures. However, the correct interpretation of zircon and monazite ages in metamorphic rocks is restricted by our limited knowledge of the behaviour of these trace minerals during metamorphism. From experimental work (e.g. Watson and Harrison 1983; Rapp and Watson 1986), it is possible to calculate the temperatures at which zircon and monazite are likely to be stable in magmas of different compositions. Recent studies by Smith and Giletti (1997), Lee et al. (1997) and Cherniak and Watson (2000) have determined the diffusion coefficients of Pb for monazite and zircon, from which U–Pb closure temperatures can be calculated. Nevertheless, there is a lack of information on the temperature at which these trace minerals begin growing during metamorphism, which stage of the rock's thermal history their U–Pb system is likely to record, and which factors influence their stability in a given metamorphic environment.

source: https://doi.org/10.7892/boris.88271 | downloaded: 12.10.2024

In this contribution, we report a systematic study of the behaviour of monazite and zircon with increasing temperature and variable rock paragenesis across a greenschist- to granulite-facies transition in the Reynolds Range (RR; northern Arunta Inlier, central Australia). We used imaging-controlled in-situ dating to ensure that metamorphic overgrowth on these accessory minerals was related to a single event and not the product of polymetamorphism. We monitored the variation in factors such as whole rock composition and melt abundance in order to determine their influence on zircon and monazite growth. In several cases, zircon and monazite from the same rocks were analysed to test for differences in U–Pb age and hence possible cooling ages recorded by monazite, which are particularly likely in a slow-cooling terrain such as the RR (Williams et al. 1996).

## Geological setting

The RR (Fig. 1) is a NW-trending mountain range in central Australia, 150 km NW of Alice Springs, which extends for over 70 km. Tectonically, it is part of the of Northern Province of the Arunta Inlier (Shaw et al. 1984). The RR consists of a polymetamorphic basement (Lander Rock Beds; dominantly pelitic and psammitic metasediments) with a sedimentary cover (Reynolds Range Group, RRG; pelitic, quartzitic and carbonatic metasediments). Numerous granitic bodies intruded both the Lander Rock Beds and the RRG, producing local contact metamorphism, before being regionally metamorphosed under low pressure–high temperature conditions (LP-HT). The RR records a metamorphic gradient from NW to SE, which has been extensively documented in both basement and cover (Dirks and Wilson 1990; Clarke and Powell 1991; Dirks et al. 1991; Hand et al. 1992; Vry et al. 1996; Buick et al. 1998). A summary of metamorphic facies and conditions is presented in Fig. 1. The deposition of the RRG post dates the granites intruding the basement at 1805 ± 3 Ma (Vry et al. 1996) and pre dates the intrusion of another granitic suite at ~1780–1790 Ma (Collins and Williams 1995).

The age of regional metamorphism in the RR has been a matter of debate. The large number of Ar–Ar and Rb–Sr age determinations carried out prior to the mid-1980s (Allen and Stubbs 1982; Black et al. 1983) scattered over a wide range (1850–300 Ma; Black and Shaw 1995; Collins and Shaw 1995), and resulted in a confusing picture of the timing of metamorphism throughout the Arunta Inlier as a whole. The first SHRIMP U–Pb dating of zircon from metamorphosed and deformed granitoids of the RR (Collins and Williams 1995) led to the conclusion that the main regional metamorphic event in the RR and the nearby Anmatjira Range occurred between 1780 and 1770 Ma. However, further SHRIMP dating of monazite and zircon from high grade metasedimentary rocks resulted in the interpretation that regional HT metamorphism in the RR occurred at 1570–1590 Ma (Vry et al. 1996; Williams et al. 1996), much later than the granitic magmatism. Williams et al. (1996) suggested that the metamorphism extended over 25 Ma with a peak at ~1594 ± 6 Ma and

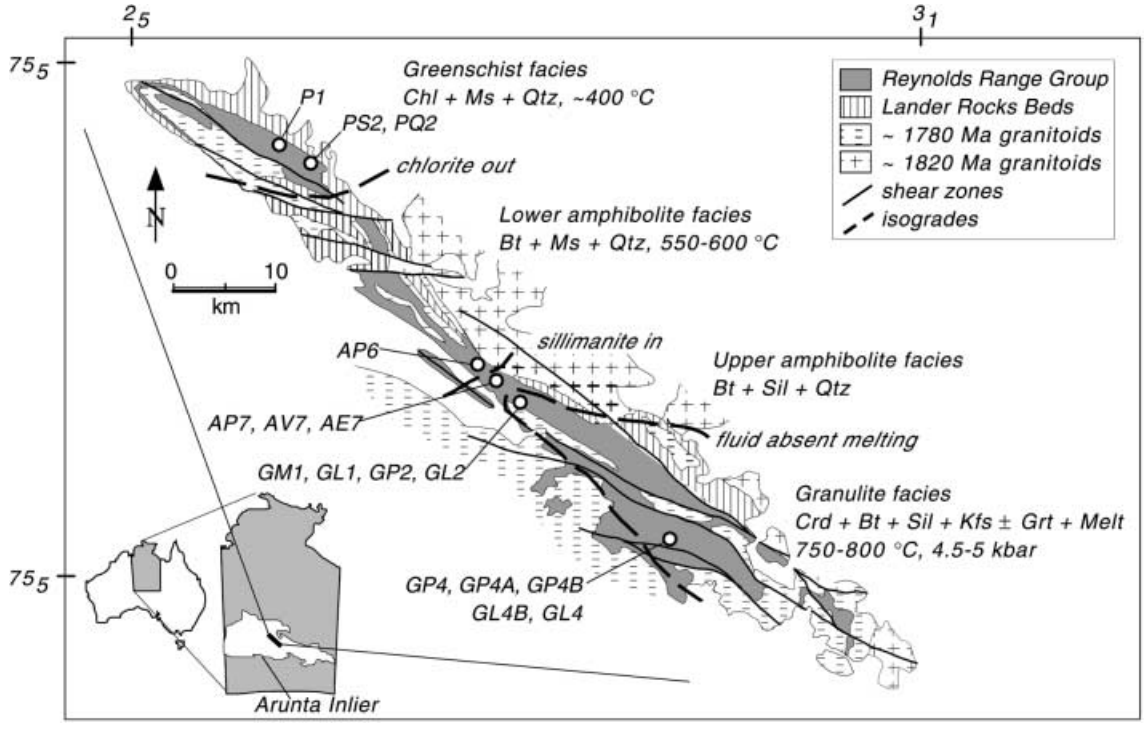


**Fig. 1** Sketch geological map of the RRG showing metamorphic isograds and sample locations. Metamorphic facies, main assemblage and P–T estimates are reported for the different metamorphic grades. Sources: Dirks et al. (1991), Clarke and Powell (1991) and Buick et al. (1998). Mineral abbreviations according to Bucher and Frey (1994)

retrogression to sillimanite–biotite facies at 1568 ± 4 Ma. This hypothesis has recently been supported by age measurements by Pb stepwise leaching of garnet (Buick et al. 1999).

## Sample description

More than 40 samples of metapelites and metapsammites of the RRG were collected along a 60-km profile along strike and across the regional metamorphic isograds (Fig. 1). Field relationships and assemblages of 14 selected samples are described briefly below in order of increasing metamorphic grade. Parageneses of the RRG metasediments along the profile are summarised in Fig. 2.

The lowest grade sample is metapelite P1, which contains intercalations of metapsammites (PS2) and metaquartzites (PQ2). Sample AP6 is an amphibolite-grade metapelite that contains pseudomorphs after earlier cordierite, which is interpreted to have grown during contact metamorphism caused by the 1780 Ma magmatism. AP7 is a sillimanite-bearing metapelite in which white mica is present only as a retrograde phase. This metapelite contains metamorphic veins (AV7 and AE7), which consists of quartz, sillimanite, white mica, tourmaline and retrograde sericite and chlorite. Because of their composition, coarse grain and field occurrence, the veins are thought to have formed through fluid flow. Metapelites GM1 and GP2 were collected at the amphibolite–granulite facies boundary, and record evidence of dehydration partial melting via the reaction biotite + sillimanite + quartz → cordierite ± K-feldspar + melt. Sample GL1 is a several metre diameter granitic pod within GM1 that contains quartz, plagioclase, K-feldspar and tourmaline. Metapelite GP2 contains small concordant leucosome interlayers that are inferred to have formed as a result of partial melting (GL2). With increasing metamorphic grade the granulites display increases in grain size and the volume of leucocratic material (inferred to be partial melt). Samples GP4, GP4A and GP4B are migmatitic granulites with abundant leucosomes forming either layers concordant to the main fabric or discordant veins in crenulations (GL4B). Locally, the leucosomes form distinct metre-scale bodies (GL4).

## Methods

Samples preserving the freshest assemblages at each metamorphic grade were selected for geochronology. Zircon and monazite were investigated by cathodoluminescence (CL) and back-scattered electron (BSE) imaging, respectively, in order to identify growth zones that possibly record different geological events. Selected domains were dated in-situ by SHRIMP ion microprobe in order to document the presence and age of overgrowths formed during the Mesoproterozoic metamorphic event and to estimate the relative amount of new growth versus detrital or inherited components.

Zircon and monazite were prepared as mineral separates, mounted in epoxy and polished down to expose the grain centres. The selection of zircons and monazites for SHRIMP analyses was done on the basis of the CL/BSE images. CL and BSE investigations were carried out at the Electron Microscope Unit at the Australian National University. CL was performed on a HITACHI S2250-N scanning electron microscope working at 15 kV, ~60 μA and ~20 mm working distance. BSE images were obtained with a Cambridge S360 scanning electron microscope using a voltage of 20 kV, variable current between 3 and 6 nA and a working distance of ~20 mm.

Zircon and monazite were analysed for U, Th and Pb using the sensitive high resolution ion microprobes (SHRIMP I and II) at the Research School of Earth Sciences. Instrumental conditions and data acquisition for zircon were generally as described by Compston et al. (1992) and Williams et al. (1996). The data were collected in sets of seven scans throughout the masses and a reference zircon was analysed each fourth analysis. The measured $^{206}Pb/^{238}U$ ratio was corrected using reference zircon from a gabbro of the Duluth Complex in Minnesota (AS3, 1099 Ma). The data were corrected for common Pb on the basis of the measured $^{204}Pb$ and assuming a Broken Hill common lead composition, which approximates the laboratory common lead at RSES.

For most of the monazite samples, data were acquired as described by Williams et al. (1996) using reduced primary beam and spot size in order to decrease the ThO ion emission. Monazite from Thompson Mine, Manitoba (1766 Ma), was used as standard material. Fractionation between $^{232}ThO^+$ and $^{238}UO^+$ was corrected by a factor calculated using the correlation between $^{232}ThO^+/^{238}UO^+$ and radiogenic $^{208}Pb/^{206}Pb$ as described by Williams et al. (1996). Even at a mass resolution of 5000, there is commonly an isobaric interference on the $^{204}Pb$, which leads to overcorrection of the Pb isotopic ratios (Fig. 3). It has been proposed (e.g. Stern and Sanborn 1998) that the size of this interference is correlated with the monazite Th content, but this was not always found to be so in the present case. In order to eliminate the interference on the $^{204}Pb$, monazite from sample AP6 was analysed using energy filtering (Ireland 1995) that discriminates against complex molecular species, which have a lower average energy than atomic ions. The monazite UO count rate was reduced by a factor of 5 by setting the energy window to remove low energy ions. With this amount of energy filtering the isobar at mass 203.97, which appears to be a complex molecule, disappeared and a normal correction for common Pb produced the expected isotopic ratios for the standard (Fig. 3). Zircon and monazite analyses were plotted on classical Concordia diagrams using the software Isoplot/Ex (Ludwig 1999). Ages were calculated at 95% confidence level on the basis of the $^{207}Pb/^{206}Pb$ isotopic ratios.

Rare earth element (REE) analysis was performed on the SHRIMP II ion microprobe applying strong energy filtering to reduce molecular interferences. Whenever possible, two isotopes for each REE were measured to check the isotopic ratios against isobaric interferences. Details of the operating conditions and data reduction are given in Hoskin (1998).

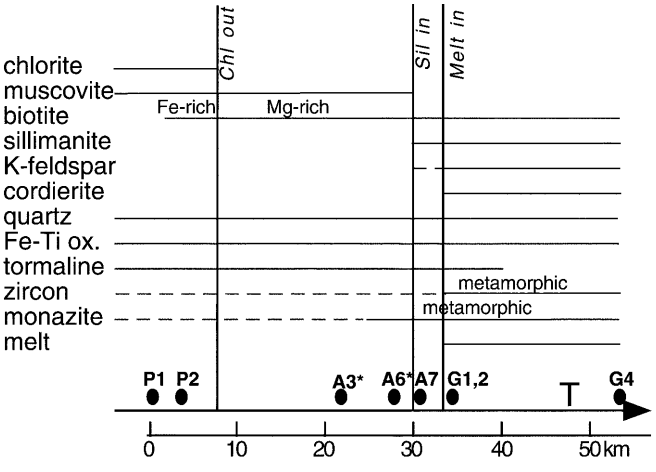


**Fig. 2** Stable parageneses of the RRG metapelites plotted against distance in order of increasing temperature. *Sample in which relics of contact metamorphic minerals are present

## Zircon response to prograde metamorphism

The samples from greenschist- to amphibolite-facies grades contain rounded zircon crystals with irregular surfaces, as typical for detrital grains. They have magmatic oscillatory zoning and yielded ages pre 1800 Ma, which is the maximum depositional age of the

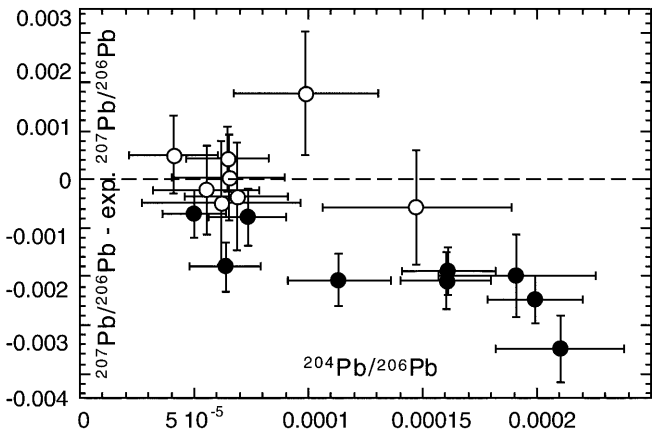


**Fig. 3** Differences between the corrected $^{207}Pb/^{206}Pb$ ratios and the expected value (0.10808) for the monazite standard plotted versus the $^{204}Pb/^{206}Pb$ ratio. Data in *black* where measured during a normal session whereas data in *white* were measured using energy filtering. Both data sets were corrected for common Pb on the base of the measured $^{204}Pb$. Energy filtering effectively eliminated the isobaric interference with $^{204}Pb$

sequence. In a few cases, unzoned metamorphic domains were detected in CL imaging, but SHRIMP dating proved these domains to be older than the known depositional age. This is evidence that zircon in these samples is exclusively detrital.

Even in localities where metamorphic veins related to fluids are present (samples AV7 and AE7) the few zircon grains found in the country rock metapelite (AP7) had no evidence of metamorphic overgrowths. The veins contain euhedral zircon grains that are spongy because of strong metamictisation, and appear to have a core-rim structure. The crystal shape and structure would suggest that this zircon is not detrital but formed during fluid infiltration. When SHRIMP analysis was attempted, the zircon showed extreme U contents (> 5000 ppm) and isotopic disturbance was so great that no age of geological significance could be obtained.

At granulite-facies grade, small overgrowths on zircon grains are present (Fig. 4). The overgrowths are from irregular to euhedral in shape and often cut across the oscillatory bands of the detrital cores. They are characterised by weak or no zoning and Th/U ratios lower than or equal to 0.1 (Supplementary Table 1). These are common features in metamorphic zircon (e.g. Williams and Claesson 1987; Williams et al. 1996; Rubatto and Gebauer 2000). It is noteworthy that the large zircon overgrowths formed in the leucosome are significantly different from magmatic zircon overgrowths found in 'S-type' granites, although the two rock types formed by a similar process. In 'S-type' granites, zircon dating the granite formation have a marked oscillatory zoning and higher Th/U ratio (≥0.3). At low granulite facies new zircon overgrowths are thin (5–30 μm) and present in only 10% of the grains or less, but with increasing metamorphic grade their thickness increases (50–100 μm) and their abundance reaches up to 80% of the grains in the restitic metapelites. In the leucosomes at any grade the overgrowths are more abundant than in the associated metapelite (cf. Fig. 4a–d) and, at the highest grades, large euhedral overgrowths are present on all zircon grains. Rounded detrital cores are often smaller in the leucosome than in the restitic metapelites suggesting that zircon resorption occurred. This is supported by the local presence of embayments in the zircon cores (Fig. 4). In some zircons, the detrital core is absent and seems to have been completely resorbed. The occurrence of the overgrowths only in the granulite facies rocks demonstrates that they formed during the regional HT metamorphism. This conclusion is in line with their absence of zoning, chemical composition (low Th/U) and similar age in the range 1562–1587 Ma (Figs. 4 and 5).

In summary, during prograde regional metamorphism in the RR, zircon does not appear to react to metamorphism at temperatures below ~700 °C. At granulite-facies conditions, where leucosomes record partial melting, zircon grew on detrital cores that are preserved up to 750–800 °C. The granulitic migmatites at the HT end of the RR have the highest abundance of new zircon overgrowths, with the leucosomes being particularly rich in new zircon. The leucosomes at these metamorphic conditions show a positive correlation between leucosome size and the volume of newly precipitated zircon. Therefore, the amount and dimension of overgrowths is roughly correlated with temperature and percentage of partial melt in the rock (Fig. 6). This conclusion agrees with the observations by Vavra et al. (1999) in the Ivrea Zone, where zircon new growth is limited to the rocks that underwent anatexis (upper amphibolite- to granulite-facies in that case) and increases with metamorphic grade.

The zircon grains in the HT leucosome GL4, which have the largest overgrowths, preserve the minimum amount of detrital cores, suggesting that new zircon formed by dissolution–precipitation. As suggested by Vavra et al. (1999), the dissolution of very fine detrital zircons via Ostwald ripening could also have been source for the new zircon growth. Our observations are consistent with the work on Zr saturation by Watson and Harrison (1983), which predicts that, for a given bulk composition, Zr solubility increases with increasing temperature. In fact, metapelites GP2 (low temperature granulite facies) and GP4A (HT granulite facies) have similar chemical compositions and Zr contents (192 and 195 ppm, respectively), but zircon overgrowths are much more abundant in the higher temperature sample. The large leucosome GL4 has bigger zircon overgrowths than the nearby leucosome GL4B. This cannot be attributed to different chemical compositions, as the partial melt was in equilibrium with the restite (see Leucosome section), which is effectively an infinite reservoir for Zr. It could indicate that the two melts formed and crystallised at different temperatures, leucosome GL4 being the higher temperature one. Alternatively, the large melt volume in GL4 favoured zircon dissolution and reprecipitation with respect to the small leucosome

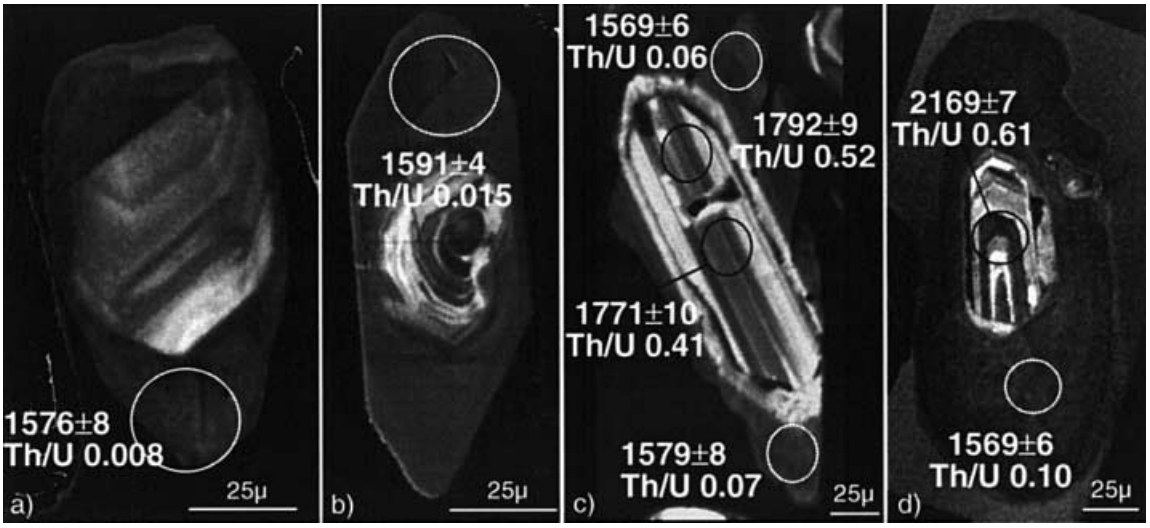


**Fig. 4** Cathodoluminescence images of zircon grains from the RR in order of increasing metamorphic grade. *Circles* indicate the SHRIMP analysis pits for which Th/U ratio and age ($^{207}Pb/^{206}Pb$ age $\pm 1\sigma$ Ma) are reported. **a** Zircon from metapelite GP2 at the amphibolite–granulite boundary. This rock contains only rare metamorphic zircon overgrowths, most of them $<25$ μm across. **b** Zircon from leucosome GL2 collected at the amphibolite–granulite boundary, which shows a large detrital core overgrown by a rather thin euhedral overgrowth dating the regional metamorphism. **c** Zircon from metapelite GP4 at higher metamorphic grade with a larger metamorphic overgrowth on a typical detrital core. **c** Zircon grain from leucosome GL4B with a small detrital core and an overgrowth significantly larger than in zircon from the coexisting metapelite GP4

vein GL4B. These conclusions are in agreement with the observation of Oliver et al. (1999) who documented variable zircon growth in different leucosome types.

The abundance of the overgrowths appears also to depend on whole rock chemistry. In fact, two samples collected within 50 m, which have the same assemblage, contain zircon grains with different degrees of overgrowth: the zircon in the more pelitic sample (GM1) has overgrowths on several grains, whereas in the sample richer in quartz (GP2) the overgrowths are very rare. Similar observations were reported by Vavra et al. (1999) for the granulites of the Ivrea Zone where metamorphic overgrowths on zircon are more abundant in metapelites than in associated meta-arenites. It is likely that the more pelitic and therefore more fertile composition of metapelite GM1 favoured a higher degree of partial melt that triggered more zircon growth than in metapsammite GP2.

## Monazite response to prograde metamorphism

No monazite could be recovered from the greenschist-facies samples from the NW of the RR, probably because of their fine grain. In fact, in thin section, small monazite grains have been found at the core of aggregates of Fe–Ti oxides (Fig. 7a) indicating that some monazite is present in the low grade rocks. Moreover, the presence of old monazite cores in the amphibolite-facies samples (see below) indicates that detrital monazite is present in this series. Therefore, monazite observed in the low grade samples is interpreted as detrital.

Unlike zircon, new crystallisation of metamorphic monazite was observed even at mid-amphibolite facies grades, before the formation of sillimanite and thus at temperatures $<650$ °C. In mid-amphibolite-facies metapelites AP6, which reached peak temperatures of 500–600 °C (Dirks et al. 1991), monazite displays a clear core-rim structure with patchy zoned cores and unzoned rims (Fig. 7b). The U–Pb analyses on monazite rims yielded a concordant age of 1576 ± 5 Ma (Fig. 8a), indicating that the rims formed during the regional metamorphism. The apparent $^{207}Pb/^{206}Pb$ ages of the cores scatter between 1610 and 2360 Ma (Supplementary Table 2). Several analyses cluster at around 1780–1790 Ma, dating the contact metamorphism that affected this rock prior to the regional event. Ages intermediate between 1580 and 1780 Ma are more likely caused by mixing between the two age components, which can occur at a very fine scale (Cocherie et al. 1998). The older cores yield a pre-deposition age and are therefore interpreted as detrital.

At higher amphibolite-facies grades within the stability field of biotite–sillimanite, small monazite grains, some of which have inclusions of sillimanite, were found in metapelite AP7 and the two metamorphic veins AE7 and AV7. Unlike the lower grade metapelite AP6, in these samples, monazite, which yields the age of the regional metamorphism (Fig. 8b), displays a rather simple zoning with no evident core-rim structure (Fig. 7c).

At granulite facies all the samples contain monazite that yields the age of the regional metamorphism (Fig. 8c–f). As with the case of zircon, monazite abundance appears to increase with increasing temperature (Fig. 6). In fact, the metapelites GP2 and GM1, which were collected close to the amphibolite–granulite boundary, contain only a few small monazite grains that are rounded and display no, or only weak zoning. The

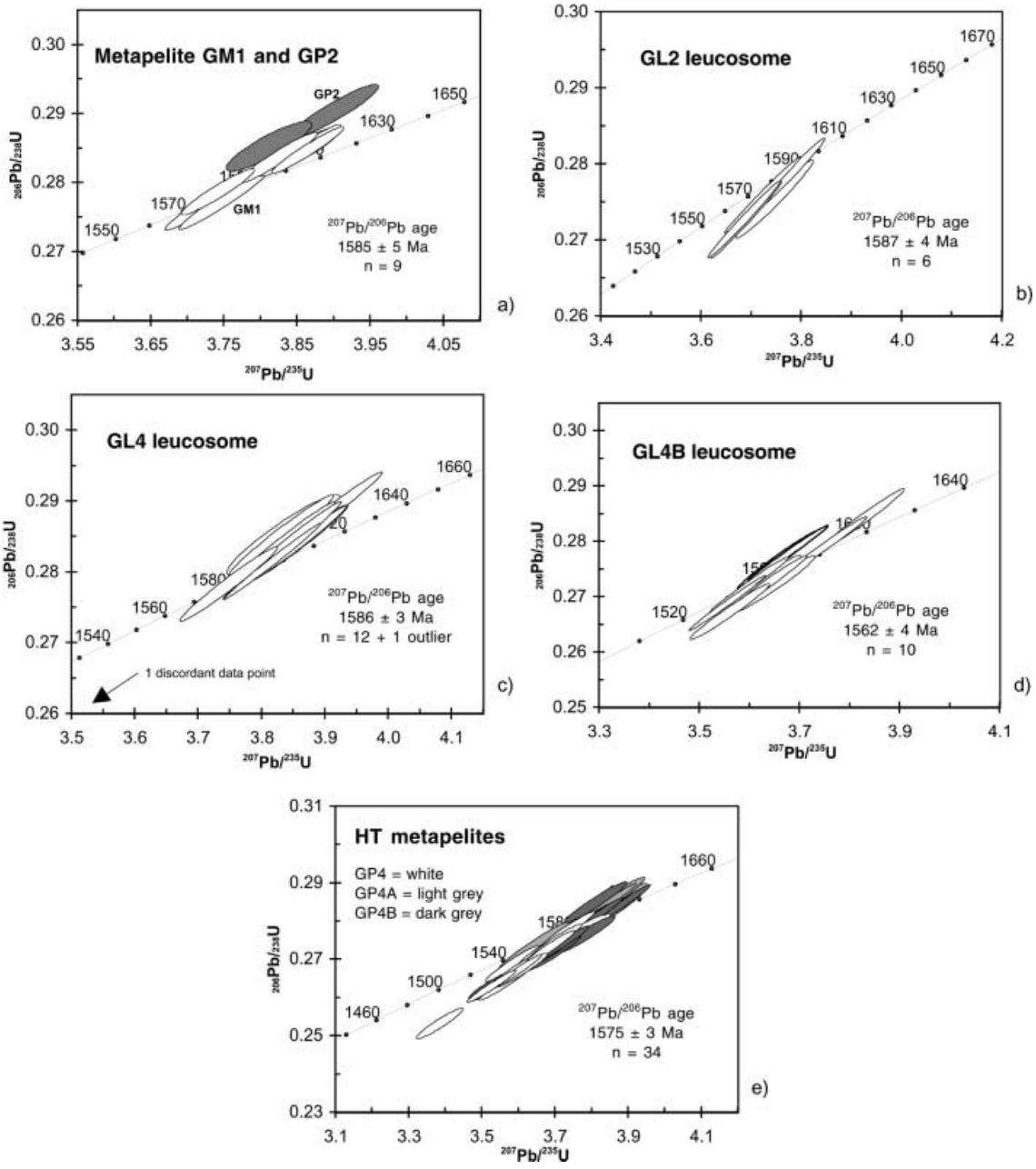


**Fig. 5** Concordia diagrams for SHRIMP U–Th–Pb analyses of zircon in the different samples in order of increasing metamorphic grade. Similar samples from the same outcrop and having the same age have been group together. Only analyses on zircon overgrowths are plotted. Mean $^{207}$Pb/$^{206}$Pb ages are given at 95% confidence level, whereas single datum points are plotted at 1$\sigma$ level

HT metapelites GP4A and GP4B contain abundant large monazite grains that display complex zoning in BSE images. They have a core-rim structure commonly with polygonal oscillatory zoning in the core (Fig. 7d). However, the U–Pb measurements did not detect, with one exception, any significant difference in age between cores and rims. Only one monazite core has a significantly older $^{207}$Pb/$^{206}$Pb age of 1617 ± 6 Ma (Supplementary Table 2). This date is thought to be a meaningless age obtained from mixing an old core with a metamorphic domain. Nevertheless, the presence of an inherited Pb component implies that the U–Pb system in monazite was not completely reset in this sample even at peak temperatures of 750–800 °C.

In monazite from the RRG granulites, BSE imaging often revealed a chemically-defined core and rim structure, which does not correspond to zoning in age. Lack of correlation between monazite chemical composition and age pattern has also been documented by Cocherie et al. (1998) at an even smaller scale. It is possible that monazite cores and rims, which have distinct chemical composition and zoning patterns, formed during different geological events, as generally observed in zircon, and that their U–Pb system was reset during the last of

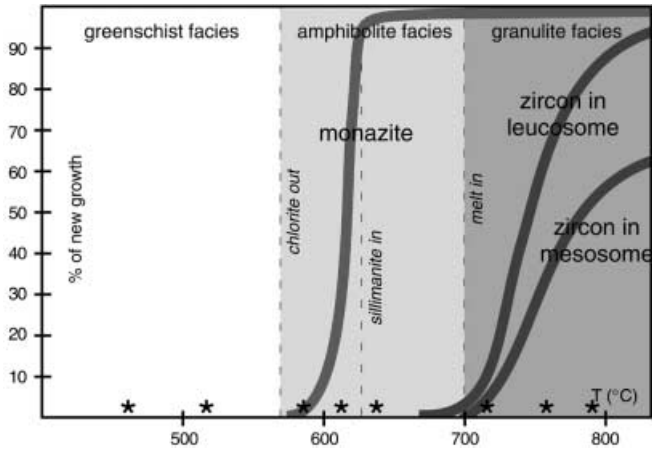


**Fig. 6** Semiquantitative diagram based on imaging and SHRIMP data representing the amount of new monazite and zircon growth with increasing metamorphic grade. For monazite no difference between leucosome and mesosome has been observed. The *stars* indicate the grade of the investigated samples

these events. This would imply that at 750–800 °C radiogenic Pb diffused out of the monazite core into the surrounding minerals (e.g. K-feldspar) or melt, whereas Th and the REE did not homogenise within the grain or diffuse out. This hypothesis would be in agreement with the experimental data on zircon that indicates that Pb diffuses at about four orders of magnitude faster than U and Th (Lee et al. 1997). Alternatively, monazite cores and rims crystallised during two different pulses of the same metamorphic event, but their age difference is not resolvable by SHRIMP dating. This second scenario has been documented by Fitzsimons et al. (1997) in leucogneisses that underwent peak metamorphism at 6–7 kbar and 800–850 °C.

In summary, in the RR metamorphic monazite, growth first occurs in the mid-amphibolite facies at around 500–600 °C, at temperatures considerably lower than for the first appearance of metamorphic zircon. Similar temperatures for the formation of metamorphic monazite were suggested by Smith and Barreiro (1990) and Kingsbury et al. (1993) who studied metapelites that underwent P–T conditions similar to the RRG. The abundance of new growth is related to temperature (Fig. 6) and, unlike zircon, the rock composition and abundance of partial melt appear not to have any influence on monazite growth. The presence of detrital monazite cores in the greenschist- and amphibolite-facies samples suggests that dissolution–reprecipitation is, at least in part, responsible for new monazite growth. Alternatively, P and light-REE could have been produced by reactions involving accessory minerals such as allanite, apatite and REE-oxides (Kingsbury et al. 1993; Bingen et al. 1996).

Inheritance of radiogenic lead in monazite can be preserved at temperatures as high as 750–800 °C. Previous studies have documented Pb inheritance in monazite in rocks that crystallised or underwent metamorphism at maximum temperatures of 700 ± 25 °C (Parrish 1990; Kingsbury et al. 1993; Cocherie et al. 1998). The slightly higher closure temperature detected here cannot be explained by fast cooling (see section on Time and duration of regional metamorphism) and, according to the experimental work of Smith and Giletti (1997), it might be caused by the relatively large diameter of the monazite crystals (50–100 μm) in the RR HT migmatitic granulites. Retention of radiogenic Pb in monazite at temperatures of 750–800 °C is better explained with the new experimental data of Cherniak et al. (2000), who established an activation energy for Pb diffusion in monazite that is higher than proposed previously.

## Leucosome – restite pairs

Zircon overgrowths in granulite-grade rocks are more abundant in the leucosomes than in the corresponding restitic metapelites. This observation is opposite to what has been observed in some other studies (e.g. Watt et al. 1996), where melt was extracted quickly and, therefore, was not in equilibrium with the source rock, and was hence poor in new zircon because of the incomplete

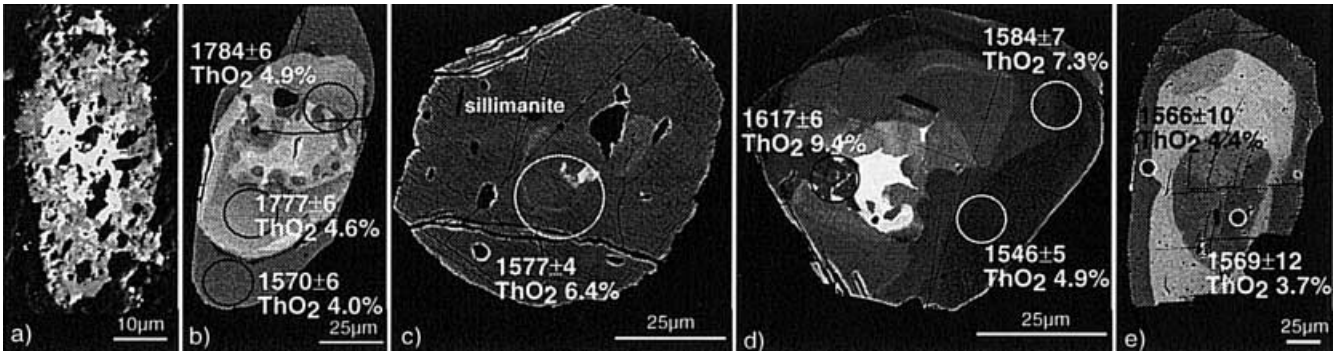


**Fig. 7** Back-scattered electron images of monazite from the RRG in order of increasing metamorphic grade. *Circles* indicate the SHRIMP analysis for which $ThO_2$ content (wt%) and age ($^{207}Pb/^{206}Pb$ age $\pm 1\sigma$ Ma) are reported. **a** Monazite (*white*) surrounded by Fe–Ti oxide found in low grade metapelite GP2. **b** Monazite in metapelite AP6 with a core recording contact metamorphism, overgrown by a rim dating the regional HT event. **c** Monazite from metapelite AP7, which formed during the regional metamorphic event, as confirmed by the needle-like inclusion of sillimanite. Note the absence of older cores and the relatively simple zoning. **d** Monazite from HT granulite GP4 that preserves inherited radiogenic Pb in the core. **e** Monazite from HT leucosome GL4B, which yielded the same age for the core and the rim

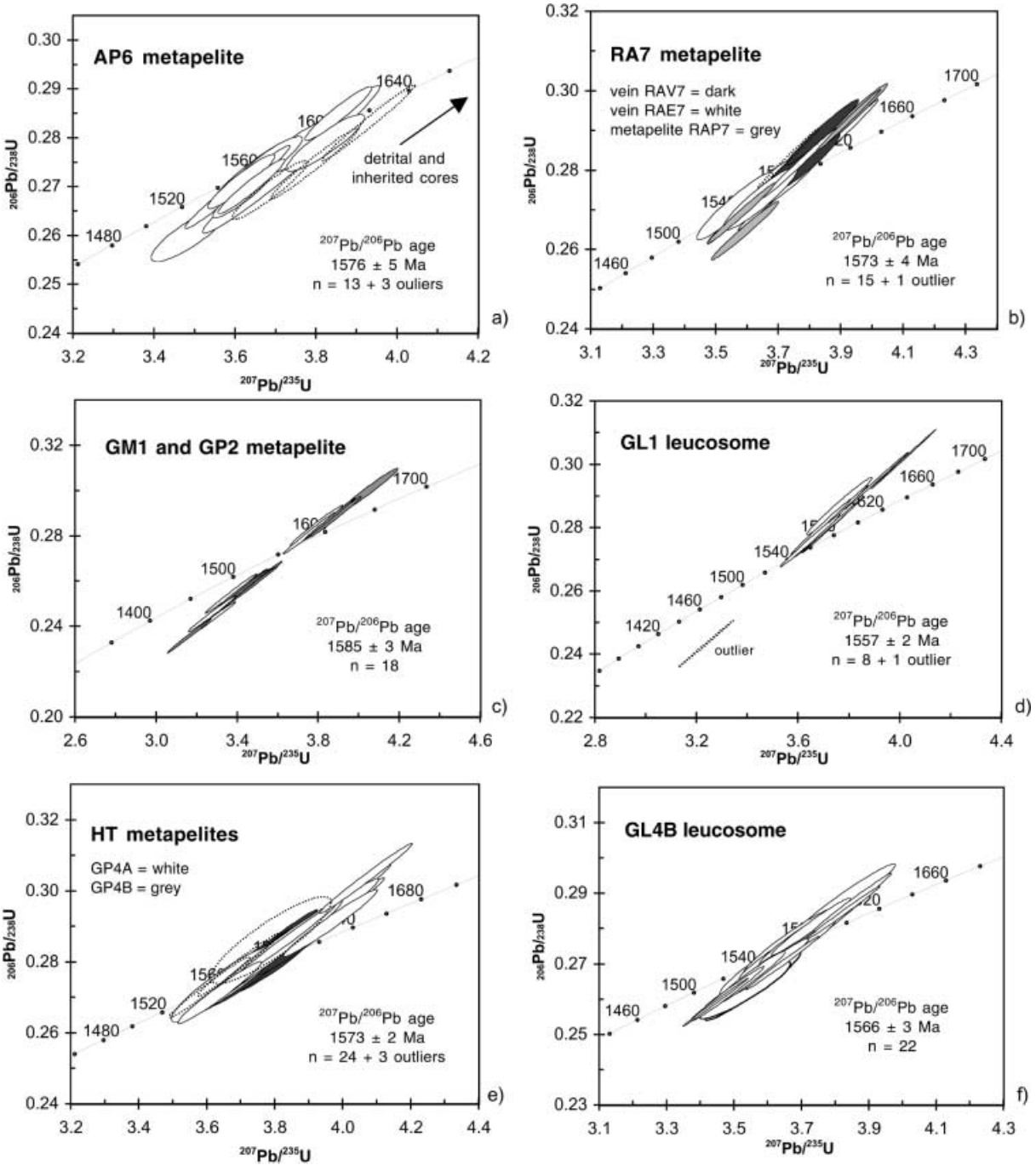


**Fig. 8** Concordia diagrams for SHRIMP U–Th–Pb analyses of monazite in the different samples in order of increasing metamorphic grade. Similar samples from the same outcrop and having the same age have been group together. Mean $^{207}Pb/^{206}Pb$ ages are given at 95% confidence level, whereas single datum points are plotted at $1\sigma$ level

dissolution of trace element-bearing accessory phases. This relationship seems not to be true for monazite, for which no correlation between rock composition and new growth has been detected in this study.

Analysis of REE has been performed on zircon overgrowths and detrital cores from the granulitic metapelite GP4 and the associated leucosome GL4B (Fig. 9). The zircon cores have highly variable REE patterns, as might be expected for a heterogeneous detrital zircon suite derived from different environments. The variability in the REE composition of the zircon cores is consistent with their $^{207}Pb/^{206}Pb$ age ranging from 1770 to 2345 Ma (Supplementary Table 1). On the other hand, the REE composition of zircon overgrowths from the restitic metapelite and its leucosome are remarkably similar: they have a steep REE pattern, a marked negative Eu anomaly and positive Ce anomaly. This parallelism suggests chemical

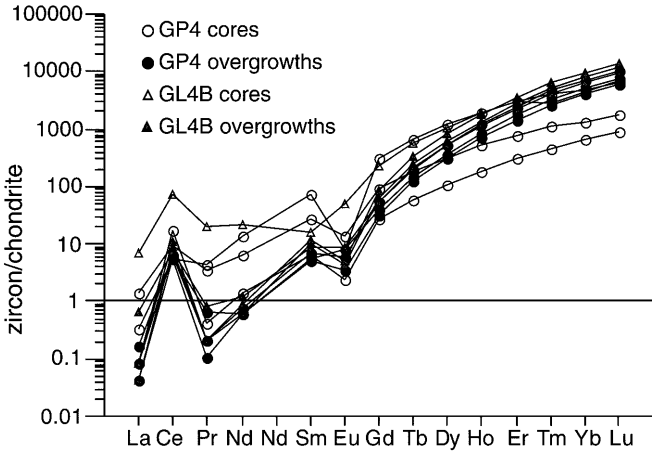


**Fig. 9** Chondrite normalised REE patterns of zircon cores and overgrowths from granulitic metapelite GP4 and associated leucosome GL4B. Detrital cores have various REE compositions, whereas metamorphic overgrowths show identical patterns indicating that chemical equilibrium between restite and melt was reached during anatexis

equilibrium between leucosome and melanosome at the time of new zircon growth (that is granulite facies), opposite to what is commonly observed in many migmatitic terrains (Watt et al. 1996). The trace element data agree with petrographic observations (small relict aggregates of quartz and feldspar are present in the restite) in indicating that not all the melt was extracted from the restitic pelites, as documented in other terrains (e.g. Cesare et al. 1997). This conclusion suggests that, even in the restites, zircon overgrowths have precipitated from a melt.

## Zircon versus monazite ages

SHRIMP analyses of the zircon overgrowths yielded Mesoproterozoic ages in the range 1562–1587 Ma with the HT metapelites and the leucosome GL4B having younger ages (1575 ± 3 and 1562 ± 4 Ma, respectively; Fig. 5). Monazite in amphibolite and granulite facies samples yielded ages in the range 1557–1585 Ma, and covered a time interval similar to that for zircon (Fig. 8). In each sample or group of samples for which zircon and monazite pairs have been dated (GM1 + GP2, GP4 and GL4B) the age yielded by the two minerals is indistinguishable. U–Pb inheritance, or a trace of it, has been documented in both minerals, indicating that the ages obtained record the formation of the overgrowth rather than the age at which the mineral/rock cooled below a certain temperature. The coincidence of the formation ages of zircon and monazite in each sample provides strong evidence that both minerals formed either at the same point in the P–T–time evolution of the rock, or at points whose age difference is within the analytical uncertainty of the age determination. There is evidence that the RR cooled over a long period of time (Williams et al. 1996; Buick et al. 1999) and even in these conditions monazite U–Pb ages do not record cooling later than zircon crystallisation.

## Time and duration of regional metamorphism

Zircon crystals in granulitic rocks of the RR have overgrowths that formed during the regional HT event. They have typical metamorphic features (irregular shape, weak zoning, low Th/U) and yield ages in the range 1562–1587 Ma (Fig. 5). In amphibolite and granulite grade rocks, monazite records the same event with ages in the range 1557–1585 Ma (Fig. 8). These data confirm a Mesoproterozoic age for the regional metamorphism in the RR in accord with previous U–Pb and Pb–Pb age determinations (Hand et al. 1995; Vry et al. 1996; Williams et al. 1996; Buick et al. 1999).

Monazite from two leucosome samples yielded the youngest ages: 1557 ± 2 Ma in leucosome GL1 and 1566 ± 3 Ma in sample GL4B. For leucosome GL4B, the young age in the monazite is confirmed in the coexisting zircon (1562 ± 4 Ma). Moreover, zircon and monazite from the HT metapelites that contain leucosome GL4B also yielded relatively young ages when compared with other samples (1575 ± 3 and 1570 ± 2 Ma, respectively). These ages are significantly younger than some of the other zircon and monazite data, including zircon from leucosomes GL2 and GL4, which were collected in the same localities. These young ages cannot be an analytical artefact because they are confirmed in different samples and in both the minerals analysed. On the other hand, the oldest ages ~1585–1590 Ma cannot be caused by mixing with older Pb components because the dating was always guided by CL or BSE imaging and all the analyses were located on metamorphic domains. In summary, the ages obtained from both zircon and monazite spread over 30 Ma, an age interval that is larger than the spread expected considering the analytical uncertainties alone. Like Williams et al. (1996), we consider this range in ages to be geologically significant.

As it appears unlikely that zircon or monazite record cooling ages throughout the terrain (see section on Zircon versus monazite ages), it is possible that in some melt segregations, and possibly in the restite in equilibrium with the melt, these minerals crystallised relatively late in the evolution of the rock unit. Zircon and monazite crystallised at the same time as final crystallisation of various melt generations or crystallised at different times during the overall melt crystallisation interval depending on rock bulk composition, melt water content and extent of melt extraction. In either case, the young ages would imply that partial melting in the RRG metapelite persisted over an extended period of time, as long as 30 Ma. During the metamorphic evolution of the RRG, partial melt first formed during prograde metamorphism at ~700 °C when the sequence crossed the reaction biotite + sillimanite + quartz ⇒ cordierite + K feldspar + melt (Vielzeuf and Holloway 1988). Then

the rocks reached peak metamorphism and started to cool below the granite solidus (Vry and Cartwright 1994; Buick et al. 1998). The data presented here suggest that during this loop partial melts were forming, segregating and crystallising continuously for 30 Ma. This is in agreement with the field observation that there exist different generations of leucosome, ranging from concordant to discordant to the main granulite-facies foliation. Although the leucosomes seem to record a protracted HT regime, in the restitic metapelite, the formation of metamorphic zircon and monazite occurred in a shorter period of time, most likely close to the thermal peak and possibly as a result of melt extraction (cf. Watt et al. 1996).

HT metamorphism lasting >25 Ma has previously been suggested by Williams et al. (1996) for the Reynolds and Anmatjira Ranges. Long lasting metamorphism has also been proposed for the Halls Creek Orogen (Oliver et al. 1999) and the Mount Isa Inlier (McLaren et al. 1999), and might prove to be a rather common feature of the Australia Proterozoic. Such a long lasting HT regime requires that the relatively high geotherm present in the RR at the time of metamorphism reached a nearly steady state. Modelling by Sandiford et al. (1998) suggested that geothermal gradients >40 °C/km and consequent long-lasting HT regimes could be induced by buried high heat producing granites. Such a geological scenario has been suggested for the long-lasting metamorphism (apparently 100 Ma) in the Mt. Isa Inlier (NW Australia; McLaren et al. 1999). A similar geological setting could have occurred in the RR if the large masses of 1780 Ma granites were buried at the base of the RRG sequence by the Middle Proterozoic. This possibility has been envisaged by Buick et al. (1998) on the basis of the modelling of Sandiford and Hand (1998).

## Conclusions

During the prograde regional metamorphism in the RR, monazite and zircon behaved in different ways. Monazite had already begun to crystallise in lower to mid-amphibolite-facies metapelites at temperatures of ~500–600 °C. During prograde metamorphism, monazite appears to progressively increase in abundance and size with increasing grade. Inheritance in the form of older cores is largely preserved at amphibolite-facies grade, but it is drastically reduced in the granulite facies rocks. However, the fact that some inherited Pb survives in the granulite-facies monazite is evidence that the closure temperature for the U–Pb system of relatively large (50–100 μm) monazites can be higher than 750–800 °C, even for very slow cooling rates.

The stability of zircon is determined by the presence of melt. Only when the metapelites reach anatexis (≥700 °C) does metamorphic zircon grow in both the restite and the leucosome, possibly after partial dissolution of pre-existing detrital zircon grains. Similar REE compositions of zircon overgrowths from metapelites and melt segregations indicate that, during anatexis, chemical equilibrium was reached between restite and melt. In zircon, the amount of new growth is a function of melt abundance (thereby temperature) and possibly influenced by whole rock composition, as more fertile rocks will reach higher degrees of partial melting. As long as melt is present, zircon and monazite crystallisation occurs, preserving a record of long lasting thermal events.

Zircon metamorphic overgrowths are distinguishable because of weak zoning in CL and are chemically different from the detrital and inherited cores. They systematically have Th/U < 0.1 and a homogeneous REE composition with steep patterns characterised by positive Ce anomaly and negative Eu anomaly. For the monazite, discrimination between metamorphic and detrital cores on the base of imaging is not always straightforward. Oscillatory zoning, as seen in zircon, is absent in monazite, where instead cores distinguished on the base of their BSE patterns commonly have no trace of inherited Pb.

The HT metamorphism in the RR was recorded in the U–Pb system of both zircon and monazite, but the different behaviour of the two minerals makes each best suited to investigating different events. In amphibolite-facies metapelites, monazite rims and cores record two metamorphic events that occurred at ~500–600 °C, of which there is no record in zircon from the same rocks. As a result, monazite is more suitable than zircon for dating relatively low temperature events. On the other hand, at HT, zircon preserves detrital or inherited cores to a much larger extent than does monazite and, therefore, zircon geochronology is particularly useful for investigating rocks that have had a polyphase thermal history. Moreover, the fact that both of these minerals can preserve Pb inheritance, or a trace of it, at HT must be remembered when multigrain or even single grain isotope dilution U–Pb dating is carried out.

**Acknowledgements** The research presented in this paper benefited greatly from discussions with Martin Hand and Jörg Hermann. The Electron Microscope Unit at the ANU is thanked for access to the SEM facilities. This project was supported by a Swiss National Foundation Postdoctoral fellowship to D.R. and by the Research School of Earth Sciences, ANU. I.S.B. acknowledges a Senior Research Fellowship from the Australian Research Council (ARC), and support from ARC Large Grant A39700909. The careful and critical comments of two anonymous reviewers greatly improved the manuscript.

## References

Allen AR, Stubbs D (1982) An $^{40}Ar/^{39}Ar$ study of a polymetamorphic complex in the Arunta Block, central Australia. Contrib Mineral Petrol 79: 319–332

Bingen B, Demaiffe D, Hertogen J (1996) Redistribution of trace elements, thorium, and uranium over accessory minerals in the course of amphibolite to granulite facies metamorphism: the role of apatite and monazite in orthogneisses from southern Norway. Geochim Cosmochim Acta 60: 1341–1354

Black LP, Shaw RD (1995) An assessment, based on U–Pb zircon data, of Rb–Sr dating in the Arunta Inlier, central Australia. Precambrian Res 71: 3–15

Black LP, Shaw RD, Stewart AJ (1983) Rb–Sr geochronology of Proterozoic events in the central and southern provinces of the Arunta Block, central Australia. Bureau Min Res, J Aust Geol Geophys 8: 129–138

Bucher K, Frey M (1994) Petrogenesis of metamorphic rocks. Springer, Berlin Heidelberg New York

Buick IS, Cartwright I, Harley SL (1998) The retrograde P–T–t path for the low-pressure granulites from the Reynolds Range, central Australia: petrological constraints and implications for low-P/high-T metamorphism. J Metamorph Geol 16: 511–530

Buick I, Frei R, Cartwright I (1999) The timing of high-temperature retrogression in the Reynolds Range, central Australia: constraints from garnet and epidote Pb–Pb dating. Contrib Mineral Petrol 135: 244–254

Cesare B, Salvioli Mariani E, Venturelli G (1997) Crustal anatexis and melt extraction during deformation in the restitic xenoliths at El Joyazo (SE Spain). Mineral Mag 61: 15–27

Cherniak DJ, Watson BE, Harrison MT, Grove M (2000) Pb diffusion in monazite: a progress report on a combined RBS/SIMS study. Eos Trans 41 Suppl, S25

Clarke GL, Powell R (1991) Proterozoic granulite facies metamorphism in the southeastern Reynolds Range, central Australia: geological context, P–T path and overprinting relationships. J Metamorph Geol 9: 267–281

Cocherie A, Legendre O, Pecaut JJ, Kouamelan AN (1998) Geochronology of polygenetic monazites constrained by in situ electron microprobe Th–U-total lead determination: implications for lead behaviour in monazite. Geochim Cosmochim Acta 62: 2475–2497

Collins WJ, Shaw RD (1995) Geochronological constraints on the orogenic events in the Arunta Inlier: a review. Precambrian Res 71: 315–346

Collins WJ, Williams IS (1995) SHRIMP ionprobe dating of short-lived Proterozoic tectonic cycles in the northern Arunta Inlier, central Australia. Precambrian Res 71: 69–89

Compston W, Williams IS, Kirschvink JL, Zhang Z, Ma G (1992) Zircon U–Pb ages for the Early Cambrian time-scale. J Geol Soc Lond 149: 171–184

Dirks PHGM, Wilson CJL (1990) The geological evolution of the Reynolds Range, central Australia: evidence for three distinct structural-metamorphic cycles. J Struct Geol 12: 651–665

Dirks PHGM, Hand M, Powell R (1991) The P–T-deformation path for a mid-Proterozoic, low pressure terrane: the Reynolds Range, central Australia. J Metamorph Geol 9: 641–661

Fitzsimons ICW, Kinny PD, Harley SL (1997) Two stages of zircon and monazite growth in anatectic leucogneiss: SHRIMP constraints on the duration and intensity of Pan-African metamorphism in Prydz Bay, East Antarctica. Terra Nova 9: 47–51

Hand M, Dirks PHGM, Powell R, Buick IS (1992) How well established is isobaric cooling in Proterozoic orogenic belts?: an example from the Arunta inlier, central Australia. Geology 20: 649–652

Hand M, Fanning M, Sandiford M (1995) Low-P high-T metamorphism and the role of high-heat producing granites in the northern Arunta Inlier. Geol Soc Australia 40: 60–61

Hoskin PWO (1998) Minor and trace element analysis of natural zircon ($ZrSiO_4$) by SIMS and laser ablation ICPMS: a consideration and comparison of two broadly competitive techniques. J Trace Microprobe Tech 16: 301–326

Ireland T (1995) Ion microprobe mass spectrometry: techniques and applications in cosmochemistry, geochemistry and geochronology. In: Hyman M, Rowe M (eds) Advances in analytical geochemistry. Greenwich, JAI Press, v. 2, pp 1–118

Kingsbury JA, Miller CF, Wooden JL, Harrison MT (1993) Monazite paragenesis and U–Pb systematics in rocks of the eastern Mojave Desert, California, USA: implications for thermochronometry. Chem Geol 110: 147–167

Lee JKW, Williams IS, Ellis DJ (1997) Pb, U and Th diffusion in natural zircon. Nature 390: 159–161

Ludwig KR (1999) Isoplot/Ex version 2.10. A geochronological toolkit for Microsoft Excel. Berkeley Geochronological Centre, Spec Publ, Berkeley, pp 1–49

McLaren S, Sandiford M, Hand M (1999) High radiogenic heat-producing granites and metamorphism – an example from the western Mount Isa Inlier, Australia. Geology 27: 679–682

Oliver NHS, Bodorkos S, Nemchin AA, Kinny PD, Watt GR (1999) Relationships between zircon U–Pb SHRIMP ages and leucosome type in migmatites of the Halls Creek Orogen, Western Australia. J Petrol 40: 1553–1575

Parrish RR (1990) U–Pb dating of monazite and its application to geological problems. Can J Earth Sci 27: 1431–1450

Rapp RP, Watson EB (1986) Monazite solubility and dissolution kinetics: implications for the thorium and light rare earth chemistry of felsic magmas. Contrib Mineral Petrol 94: 304–316

Rubatto D, Gebauer D (2000) Use of cathodoluminescence for U–Pb zircon dating by ion microprobe: some examples from the Western Alps. In: Pagel M, Barbin V, Blanc P, Ohnenstetter D (eds) Cathodoluminescence in geosciences. Springer, Berlin Heidelberg New York, pp 373–400

Sandiford M, Hand M (1998) Australian Proterozoic high temperature, low pressure metamorphism on the conductive limit. In: Treloar PJ, O'Brien PJ (eds) What drives metamorphism and metamorphic reactions? Geol Soc Lond, Spec Publ, London, pp 109–120

Shaw RD, Stewart AJ, Black LP (1984) The Arunta Inlier: a complex ensialic mobile belt in central Australia. Part 2: tectonic history. Aust J Earth Sci 31: 457–484

Smith HA, Barreiro B (1990) Monazite U–Pb dating of staurolite grade metamorphism in pelitic schists. Contrib Mineral Petrol 105: 602–615

Smith HA, Giletti BJ (1997) Lead diffusion in monazite. Geochim Cosmochim Acta 61: 1047–1055

Stern R, Sanborn N (1998) Monazite U–Pb and Th–Pb geochronology by high-resolution secondary ion mass spectrometry (SHRIMP). Radiogenic age and isotopic studies: report 11. Geol Survey Canada, Ottawa, 1998-F

Vavra G, Schmidt R, Gebauer D (1999) Internal morphology, habit and U–Th–Pb microanalysis of amphibolite-to-granulite facies zircons: geochronology of the Ivrea Zone (Southern Alps). Contrib Mineral Petrol 134: 380–404

Vielzeuf D, Holloway JR (1988) Experimental determination of the fluid-absent melting relations in the pelitic system. Contrib Mineral Petrol 98: 257–276

Vry JK, Cartwright I (1994) Saphirrine–kornerupine rocks from the Reynolds Range, central Australia: constraints on the uplift history of a Proterozoic low pressure terrain. Contrib Mineral Petrol 116: 78–91

Vry J, Compston W, Cartwright I (1996) SHRIMP II dating of zircons and monazites: reassessing the timing of high-grade metamorphism and fluid flow in the Reynolds Range, northern Arunta Block, Australia. J Metamorph Geol 14: 335–350

Watson BE, Harrison MT (1983) Zircon saturation revisited: temperature and composition effects in a variety of crustal magma types. Earth Planet Sci Lett 64: 295–304

Watt GR, Burns IM, Graham GA (1996) Chemical characteristics of migmatites: accessory phase distribution and evidence for fast melt segregation rates. Contrib Mineral Petrol 125: 100–111

Williams IS, Claesson S (1987) Isotopic evidence for Precambrian provenance and Caledonian metamorphism of high grade paragneisses from the Seve Nappes, Scandinavian Caledonides. II. Ion microprobe zircon U–Th–Pb. Contrib Mineral Petrol 97: 205–217

Williams IS, Buick IS, Cartwright I (1996) An extended episode of early Mesoproterozoic metamorphic fluid flow in the Reynolds Range, central Australia. J Metamorph Geol 14: 29–47